Environmental Toxicology and Chemistry—Volume 38, Number 11—pp. 2447–2458, 2019
Received: 5 April 2019 | Revised: 2 May 2019 | Accepted: 30 July 2019

Environmental Toxicology

Hyporheic Interactions Increase Zinc Exposure and Effects on *Hyalella azteca* in Sediments under Flow-Through Conditions

Anna M. Harrison,* Michelle L. Hudson, and G. Allen Burton, Jr.

School for Environment and Sustainability, University of Michigan, Ann Arbor, Michigan, USA

Abstract: Groundwater–surface water interactions in the hyporheic transition zone can influence contaminant exposure to benthic macroinvertebrates. In streams, hyporheic flows are subject to varying redox conditions, which influence biogeochemical cycling and metal speciation. Despite these relationships, little is known about how these interactions influence the ecological risk of contaminants. The present study investigated the effects of hyporheic flows and zinc (Zn)-contaminated sediments on the amphipod *Hyalella azteca*. Hyporheic flows were manipulated in laboratory streams during 10-d experiments. Zinc toxicity was evaluated in freshly spiked and aged sediments. Hyporheic flows altered sediment and porewater geochemistry, oxidizing the sediments and causing changes to redox-sensitive endpoints. Amphipod survival was lowest in the Zn sediment exposures with hyporheic flows. In freshly spiked sediments, porewater Zn drove mortality, whereas in aged sediments simultaneously extracted metals (SEM) in excess of acid volatile sulfides (AVS) normalized by the fraction of organic carbon (*f*OC) [(SEM-AVS)/*f*OC] influenced amphipod responses. The results highlight the important role of hyporheic flows in determining Zn bioavailability to benthic organisms, information that can be important in ecological risk assessments. *Environ Toxicol Chem* 2019;38:2447–2458. © 2019 SETAC

Keywords: Hyporheic zone; Groundwater–surface water transition zone; Sediment toxicity; Metal bioavailability; Environmental risk assessments

INTRODUCTION

Groundwater–surface water interactions influence most lotic ecosystems, but their effects on contaminant bioavailability remain largely unstudied. Previous work has demonstrated the importance of groundwater–surface water interactions in determining the toxicity and bioaccumulation of chlorobenzenes for caged *Ceriodaphnia dubia*, *Hyalella azteca*, *Chironomus tentans*, and *Lumbriculus variegatus* (Greenberg et al. 2002). The caged test organisms exposed to sediments had higher survival and lower chlorobenzene bioaccumulation at a site with downwelling hyporheic flow compared with sites without dominant hyporheic flow direction, despite higher porewater chlorobenzene concentrations at the downwelling site. Organism responses to chlorobenzene could not have been predicted without knowledge of these hyporheic flow conditions. Because benthic macroinvertebrates are used to set standards for contaminant toxicity, a better understanding of effects from hyporheic flows is needed for risk assessments.

Ecological risk assessments for metals, in particular, may benefit from measurements of hyporheic flow, because hyporheic flows influence sediment redox chemistry and pH (Hendricks 1993; Franken et al. 2001), which in turn affect metal speciation and binding (Calmano et al. 1993). In streams, upstream riffles are typically dominated by downwelling of surface waters into sediments and are more oxidized than downstream riffles, which are dominated by upwelling of more reduced hyporheic waters from the sediments (Boulton 1993; Brunke and Gonser 1997; Hendricks and White 2000; Olsen and Townsend 2003; Figure 1).

Under physically and chemically stable conditions, divalent metals like zinc (Zn) are likely to bind to various ligands in sediments, decreasing their bioavailability to biota. The likelihood of ligand binding is related to the redox chemistry in the sediments. In anoxic sediments, sulfide is an important binding ligand. Organic carbon is an important binding ligand in both anoxic and oxic sediments (Calmano et al. 1993; Chapman et al. 1998). Iron (Fe) and manganese (Mn) oxide minerals offer a binding site for divalent metals under oxic conditions (Costello et al. 2015; Danner et al. 2015; Mendonca et al. 2017), which has been an

This article includes online-only Supplemental Data.
* Address correspondence to harri25a@cmich.edu
Published online 1 August 2019 in Wiley Online Library (wileyonlinelibrary.com).
DOI: 10.1002/etc.4554

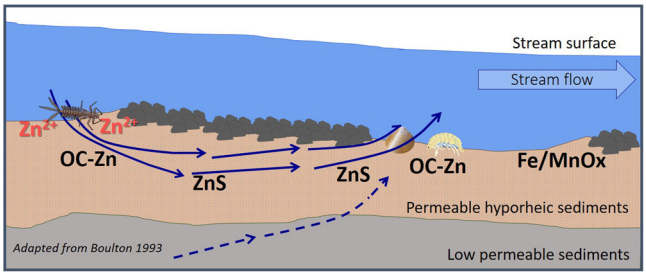

FIGURE 1: Lateral view of the hyporheic zone at the groundwater-surface water interface with hypothesized relationships between hyporheic flows and Zn bioavailability. Shallow hyporheic flow paths (solid blue lines) are dominated by local variability in stream gradient and bedform (e.g., pools, riffles). Groundwater contributes to the hyporheic zone via longer flow paths (dashed blue lines). Oxygenated downwelling zones on the riffle's upstream end may have greater bioavailable Zn (red text) than less-oxygenated upwelling zones on the riffle's downstream end, where Zn is more likely bound to sulfide and organic carbon (black text). Fe and Mn oxide minerals are also possible binding ligands in shallow oxic sediments.

important binding ligand in the hyporheic zone (Harvey and Fuller 1998). Thus, sulfide and organic carbon may be important binding ligands in more reduced upwelling zones, whereas Fe and Mn oxide complexes may be a critical binding ligand in oxidized sediments characteristic of downwelling zones.

Despite evidence of the importance of hyporheic flows on contaminant exposure to benthic macroinvertebrates and ecological risk, hyporheic zones are generally unaccounted for in ecological risk assessments. Field research has demonstrated some effects of hyporheic flows on metal contaminant exposure and effects. Microbial communities of the hyporheic zone in mining-impacted streams exhibited effects from metals on functional group structure (Feris et al. 2003, 2009). Macroinvertebrate communities were most diverse in metal-contaminated field sediments that had high hydraulic conductivity and high filtration of surface water into the streambank, essentially diluting metals within the hyporheic zone sediments (Gibert et al. 1995), similar to the relationship between chlorobenzene and downwelling observed in Greenberg et al. (2002). Macroinvertebrate communities in the hyporheic zone also responded to metal contamination (Nelson and Roline 1999; Moldovan et al. 2011), but research is limited that mechanistically links hyporheic flows to metal concentrations and biotic effects.

To assess the impacts of hyporheic flows in metal-contaminated sediment, artificial stream experiments in the laboratory can assist with understanding metal exposure and effects under controlled conditions. By eliminating many confounding variables present in the field, laboratory experiments can identify mechanisms of effects among physical processes, sediment chemistry, and biological endpoints. Laboratory flume experiments showed effects of passive hyporheic flows on metal chemistry (Zaramella et al. 2006) and effects of sedimentation on interstitial spaces in the hyporheic zone (Rehg et al. 2005). Mesocosm experiments also showed the importance of both upwelling and downwelling zones for amphipod presence in systems with excess sedimentation (Mathers et al. 2014). This body of work has indicated the importance of hyporheic flows on both metals and invertebrates, yet there is limited research to connect sediment metal chemistry to ecological effects in the hyporheic zone.

Our study assessed the influences of oxidized hyporheic flows on Zn bioavailability and effects on *H. azteca* in Zn-amended sediment. We hypothesized that oxidized hyporheic flows would release more bound Zn from sediments, compared with exposures without hyporheic flow. Such Zn release would increase exposure and potentially cause adverse effects on *H. azteca*. We also hypothesized that over time Zn concentrations would stabilize and become less toxic to *H. azteca*.

MATERIALS AND METHODS

Sediment selection and spiking

Sediment was collected from an upstream reference reach of Little Black Creek in Muskegon Heights, Michigan, USA (43.216062 N, 86.180030 W). The outlet of Little Black Creek is a US Environmental Protection Agency (USEPA) Area of Concern due to metal contamination from a Zn smelting operation (Cooper et al. 2001; Steinman et al. 2003), with documented concentrations above probable effects concentrations (PECs; MacDonald et al. 2000). The sediment is sandy, allowing for hyporheic exchange during the mesocosm experiments. Little Black Creek sediment is low in sulfide and organic carbon and has moderate to high Fe concentrations (Table 1). Sediment was collected from Little Black Creek and purged with N_2 gas before being sealed and stored for 1 mo. Half of the sediment was amended with zinc chloride ($ZnCl_2$), to obtain total Zn concentrations above the PEC for Zn (459 mg/kg). Once amended with Zn, sediments were rolled twice weekly for 30 d (Simpson et al. 2004), and the pH was slightly adjusted with NaOH to raise the pH to within 0.3 pH units of the original sediments, approximately 7.3 (Hutchins et al. 2009).

Experimental design

Twelve flow-through artificial streams (flumes) were used to examine the effects of oxidized hyporheic flows on Zn exposure to *H. azteca* (Supplemental Data, Figure S1). The flumes were constructed from 0.5-inch-thick clear acrylic (Figure 2). Surface water and hyporheic water inputs were both sourced from Ann Arbor (MI, USA) municipal water after passing through activated carbon cartridges and a biofiltration tank. Water was delivered to 2 separate manifold systems with 12 water supply ports each (1 for each flume). One manifold supplied surface water to each flume, and the second manifold supplied hyporheic flows to each flume. Surface water flowed at 2.5 cm^3/s and entered each flume through a holding tank on the upstream end of the flume. Water flowed over a spillover dam to provide surface water to the exposures in the main chamber of the flume without sediment disturbance. Hyporheic flows were set at 0.46 cm^3/s (or 0.15 cm/min velocity), to simulate shallow, low-residence-time hyporheic flow. The flow rates were high enough to supply surface and hyporheic water continuously to the sediments, but low enough to prevent erosion or movement of sediments. The hyporheic flow rates were established

TABLE 1: Sediment chemical properties during the initial and aged experiments for reference (Ref) and zinc-amended (Zn) sediments under hyporheic (Hyp) and nonhyporheic (nonHyp) flow treatments

Sediment-hyporheic	Experiment	pH[a,b]	*f*OC[c] (% C)	AVS (μmol g^{-1})	(SEM-AVS)/*f*OC (μmol g^{-1})[c]	Fe (g kg^{-1})	Mn (mg kg^{-1})	Zn (mg kg^{-1})
Reference	Pre-exposure	7.31	0.68	1.04	–139.1	5.4	42.1	7.6
Zinc	Pre-exposure	7.04	0.57	0.80	–33.3	3.8	37.7	425.9
Ref-nonHyp	Initial at day 10	7.67 ± 0.02	1.28 ± 0.65	0.78 ± 0.25	–101.5 ± 132.0	5.11 ± 0.4	39.8 ± 2.7	7.0 ± 0.7
Ref-Hyp	Initial at day 10	7.78 ± 0.04	0.71 ± 0.06	0.34 ± 0.10	–36.6 ± 34.2	5.44 ± 0.4	35.1 ± 2.4	8.2 ± 0.9
Zn-nonHyp	Initial at day 10	7.60 ± 0.04	0.52 ± 0.09	0.56 ± 0.08	1172.4 ± 326.8	4.15 ± 0.1	36.4 ± 0.5	420.7 ± 11.8
Zn-Hyp	Initial at day 10	7.92 ± 0.06	0.36 ± 0.04	0.36 ± 0.06	1272.6 ± 363.0	4.28 ± 0.2	28.2 ± 1.5	378.7 ± 17.5
Ref-nonHyp	Aged at day 10	7.29 ± 0.06	0.68 ± 0.05	0.44 ± 0.14	–50.6 ± 29.8	6.21 ± 0.4	53.6 ± 3.7	15.5 ± 1.2
Ref-Hyp	Aged at day 10	7.22 ± 0.06	1.10 ± 0.32	0.09 ± 0.09	–6.2 ± 20.8	7.12 ± 1.1	46.1 ± 5.4	15.4 ± 1.5
Zn-nonHyp	Aged at day 10	7.19 ± 0.05	0.53 ± 0.13	0.43 ± 0.04	1113.6 ± 457.6	4.42 ± 0.4	34.3 ± 3.2	405.9 ± 30.4
Zn-Hyp	Aged at day 10	7.20 ± 0.05	0.34 ± 0.01	0.44 ± 0.14	1555.5 ± 430.6	4.32 ± 0.2	29.1 ± 2.9	405.6 ± 24.6

[a]pH was measured in the porewater.
[b]For pH, the aged experiment values are from day 5, not day 10.
[c]Loss-on-ignition values were used to calculate *f*OC.
*f*OC = fraction of organic carbon; AVS = acid volatile sulfides; SEM = simultaneously extracted metals; Fe = total sediment iron; Mn = total sediment manganese; Zn = total sediment zinc.

primarily from the potential groundwater loading velocities at the site the sediments were collected (2.0 m/d or 0.14 cm/min; Baker et al. 2003). Other studies have documented infiltration rates of 0.2 cm/min in sandy hyporheic sediments (i.e., <2 mm) of headwater streams (Munn and Meyer 1988), and hyporheic sediments dominated by sand with intermediate hydraulic conductivity averaged 0.072 cm/min (Morrice et al. 1997). Both water sources flowed continuously during the experiments.

Each flume had one sediment exposure, either Zn-spiked (Zn) or reference (Ref), and 2 separate hyporheic exposures, hyporheic inputs (Hyp) and no hyporheic inputs (nonHyp). The 4 experimental treatments were: Zn-Hyp, Zn-nonHyp, Ref-Hyp, and Ref-nonHyp. Six flumes contained reference sediments, and 6 flumes contained Zn-spiked sediments. In each flume, 2 sediment baskets (200 cm^2 surface area, 8.3 cm deep) with open sides were used as the amphipod exposure units. Each basket was lined with mesh, filled with exposure sediments, and placed in the artificial streams with sand as a filler substrate (Figure 2). Within each flume (reference or Zn sediment), there were 2 baskets with the same sediment and different hyporheic exposures for 6 replicates/experimental treatment. To prevent effects of hyporheic inputs into the shared surface water, the upstream sediment exposure basket was a nonhyporheic exposure, and the downstream exposure basket had a hyporheic input. Hyporheic water was delivered to the flume through a long, flat, porous airstone buried at the bottom of the sediment exposure basket on the downstream basket in each flume. Hyporheic water was pushed through the porous stone, into the overlying sediments and ultimately into the surface water.

Two 10-d experiments were performed on the same sediments with the same hyporheic conditions. An initial experiment (days 0–10) took place before sediment aging under flow-through conditions, and a second aged experiment took place approximately 80 d later (days 82–92). Aging of sediment under flow-through conditions has been shown to decrease the toxicity of copper to *H. azteca* (Costello et al. 2015). Between experiments, sediments were continuously inundated with overlying water, which was renewed twice each week, but surface water did not flow continuously. Hyporheic flow was not present between experiments.

Chemistry sampling

Porewater sampling ports located laterally along each flume allowed for porewater sampling at 1.5-cm depth

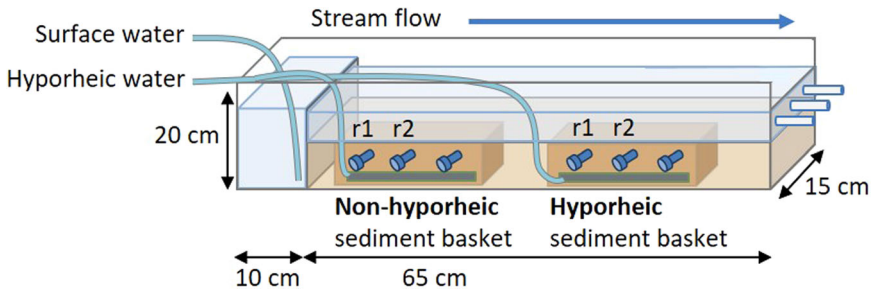

FIGURE 2: Lateral view of a singular experimental stream (flume). Each of the 12 experimental streams was set up with the same surface and hyporheic flows. Six flumes contained reference sediments in both exposure baskets, and 6 flumes contained Zn-spiked sediments in both baskets. Both the upstream sediment basket (nonhyporheic) and downstream basket (hyporheic) had 3 rhizon sampling ports, and porewater was extracted from ports r1 and r2.

throughout the experiment (Figure 2). Porewater was extracted via rhizon samplers (0.19-μm filters). During the initial experiment, porewater was sampled on days 0, 1, 3, 5, 7, and 10. In the aged experiment, porewater was sampled on days 0, 2, 5, and 9 (or in total days: 82, 84, 87, and 91). From rhizon port-1, an 11-mL porewater sample was extracted and measured for dissolved oxygen (YSI Professional Plus ODO), pH (Thermo Scientific Orion Star A121 device), and temperature within 10 min of sample collection. Prior to water quality measurements, 1 mL was extracted to measure reduced iron (Fe^{2+}), a redox indicator, using the ferrozine method (Stookey 1970; Kostka and Luther 1994). It is assumed that Fe^{2+} is inversely related to dissolved oxygen. Absorbance was measured on a spectrometer (Thermo Scientific Genesys 10 UV scanning) the same day. From rhizon port-2, 10 mL of porewater was extracted and acidified with trace metal grade nitric acid to 2% for analysis of dissolved metals (Zn, Fe, and Mn) by inductively coupled plasma–optical emission spectrometry (ICP–OES by PerkinElmer). On each sampling day, one surface water sample per flume was collected using a syringe, filtered on a 0.45-μm Millipore syringe-attached filter, and acidified to 2% nitric acid for dissolved metal analysis on an ICP–OES device. Blanks (Milli-Q water) were collected and acidified on each sampling day, and sample metal concentrations were corrected for blank values. The ICP–OES detection limits were 50 μg/L for Fe, 25 μg/L for Mn, and 10 μg/L for Zn. Six replicate porewater samples were collected each sampling day for all 4 treatment types.

Sediments were sampled at the beginning and end of both experiments. In the initial experiment, samples of both sediment types were frozen and stored on sediment deployment, and then sediment cores were taken from each flume-basket on day 10. In the aged experiments, sediment cores were taken from each flume-basket on days 81 and 92. For each experiment, 24 cores were extracted with 6 replicates for each of the 4 treatments. All sediment cores were taken using a 60-mL syringe (sawed to create a coring tube), and then stored in a 50-mL centrifuge tube; the headspace was purged with N_2 gas, and the cores were stored frozen. Sediment samples were later thawed for acid volatile sulfide (AVS) and simultaneously extracted metals (SEM) analysis (Allen et al. 1991; 4 replicates/treatment), Fe oxide content (total, amorphous, and crystalline; 3 replicates/treatment; Kostka and Luther 1994), dried for total metals (Zn, Fe, and Mn), and combusted for the fraction of organic carbon (*f*OC) via loss-on-ignition (6-h combustion at 450 °C). For total metal digestion, 0.5 g of dried sediment was digested in 7 mL of trace metal grade nitric acid in a Hot Block (Environmental Express) at 112 °C for 100 min according to USEPA method 3050B (US Environmental Protection Agency 1996), and then diluted 50 times for analysis by ICP–OES. During the digestion, metal concentrations were corrected for the sample analysis process using a procedural blank (Milli-Q water). Metal recovery from the digestion was verified (>80%) by including standard reference sediment in the digestion. Iron oxide content was measured by ICP–mass spectrometry (MS).

Biological sampling

In both experiments, 7- to 14-d-old *H. azteca* were exposed to sediment and hyporheic conditions in each flume-basket. Ten *H. azteca* were placed into a small plastic exposure chamber with 250-μm mesh on one side, to allow for surface water and sediment exposure to organisms (Costello et al. 2015). Endpoints for *H. azteca* included survival and growth.

Statistical analyses

Data analysis was performed in RStudio Ver 1.1.453 (RStudio Team 2018). Linear mixed-effects models using the packages lme4 (Bates et al. 2015) and lmerTest (Kuznetsova et al. 2017) were used to assess effects over time on porewater chemistry of both factors (Zn amendment and hyporheic flow presence). Main effects included sediment (Zn-spiked vs reference), hyporheic flow (hyporheic vs nonhyporheic), and time (as a continuous variable), with flume as a random effect. All 2-way interactions between the 3 main effects were included in the models. Two-way interactions between sediment type and hyporheic flow tested for variation in porewater chemistry between the 2 sediments (Zn and reference) caused by the hyporheic treatment. Two-way interactions between time and hyporheic flow tested for variation in porewater chemistry between the 2 hyporheic exposures over time. Two-way interactions between time and sediment tested for differences in porewater chemistry between sediment types over time. Main effects were only assessed in the results when factors were not involved in interactions with one another, although main effects are reported. Porewater variables with right skewed distributions were log-transformed for model analysis (porewater Fe^{2+}, Fe, Mn, and Zn in the initial experiment and porewater Mn and Zn in the aged experiment).

Sediment chemistry endpoints with only one sampling time point (total metals, SEM-AVS, organic carbon, Fe/Mn oxides) were assessed using linear mixed-effects models. Main effects in the model included hyporheic flow and Zn-spiked sediment, with flume as the random effect. Interactions tested for variation in sediment chemistry between the 2 sediments caused by hyporheic flows.

Effects of hyporheic flow and Zn-spiked sediment treatments on *H. azteca* survival were analyzed using generalized linear mixed-effects models (with binomial distribution) with flume as a random effect. Post hoc tests of treatment-level differences were conducted using the multcomp package with a Holm correction for multiple comparisons (Hothorn et al. 2008). Correlation analyses assessed the relationships between continuous porewater and sediment chemistry parameters and biological parameters.

RESULTS

Initial sediment experiment

Porewater dissolved oxygen increased slightly in nonhyporheic exposures over time, but no changes in hyporheic exposures were observed over the 10 d ($p = 0.043$; Table 2). Nonhyporheic exposures had lower overall dissolved oxygen

TABLE 2: Initial experiment linear mixed effects model results for effects of time, hyporheic flow, and Zn-amendment on porewater and sediment chemistry[a]

	Main effects			Interactions		
Endpoints	Time	Hyporheic	Zn	Time × Hyp	Time × Zn	Hyp × Zn
Porewater DO	(+) 1.290	(+) 5.323***	(–) 0.036	2.048*	0.905	0.226
Porewater Fe^{2+}[b]	(–) 0.917	(–) 10.584***	(–) 5.296***	1.340	2.668**	0.362
Porewater pH	(+) 6.919***	(+) 0.832	(–) 4.655***	1.000	3.189**	5.618***
Porewater Fe[b]	(–) 0.179	(–) 6.755***	(–) 4.752***	2.987**	1.285	3.208**
Porewater Mn[b]	(–) 1.088	(–) 5.702***	(+) 1.347	3.369**	0.405	2.277*
Porewater Zn[b]	(+) 6.484***	(+) 1.045	(+) 27.111***	0.458	8.983***	4.920***
Total Fe	NA	(+) 0.846	(–) 3.020**	NA	NA	0.363
Total Mn	NA	(–) 1.851	(–) 2.698*	NA	NA	0.954
Total Zn	NA	(+) 0.081	(+) 27.136***	NA	NA	2.234*
Zn_{SEM}-AVS/*f*OC	NA	(–) 0.609	(+) 9.796***	NA	NA	–0.235
Zn_{SEM}	NA	(–) 0.139	(+) 13.882***	NA	NA	2.700*
AVS	NA	(–) 2.358*	(+) 0.104	NA	NA	0.906
*f*OC	NA	(–) 1.328	(–) 0.821	NA	NA	0.672

[a]The *t* value and significance levels are reported, along with a (+) or (–) to indicate effects directions of main effects (i.e., positive or negative effect of time, hyporheic flow, or Zn-spiked sediment).
[b]Variables were log-transformed due to non-normal distributions.
*$p < 0.05$.
**$p < 0.01$.
***$p < 0.001$.
DO = dissolved oxygen; Zn_{SEM} = zinc fraction of simultaneously extracted metals; AVS = acid volatile sulfides; *f*OC = fraction of organic carbon; NA = not applicable.

than hyporheic exposures and increased 27.8% over the 10 d, from 3.09 ± 0.24 mg/L (mean ± standard error [SE]) on day 1 to 3.94 ± 0.22 mg/L on day 10. Hyporheic exposures only increased by 4.3%, ranging from 4.46 ± 0.21 mg/L on day 1 to 4.65 ± 0.18 mg/L on day 10 (Figure 3A). There was no effect of sediment treatment on dissolved oxygen ($p = 0.97$).

Overall, Fe^{2+} was higher in the nonhyporheic exposures compared with the hyporheic exposures ($p < 0.001$; Table 2), as expected from dissolved oxygen concentrations. In both hyporheic exposures, Fe^{2+} remained near 0.00 mg/L throughout most of the experiment, indicating near complete oxidation caused by the hyporheic treatment. On day 10, Fe^{2+} in the Ref-Hyp exposure was 98.9% lower than in Ref-nonHyp (0.15 ± 0.13 and 13.29 ± 1.97 mg/L, respectively), and the Zn-Hyp exposure had Fe^{2+} concentrations that were 90.7% lower than Zn-nonHyp (0.28 ± 0.25 mg/L and 2.96 ± 0.48 mg/L, respectively; Figure 3B). Relative to initial concentrations, Fe^{2+} in the Zn-spiked sediment treatments increased more over the 10 d, compared with reference sediments ($p = 0.019$; Table 2). The Zn-spiked sediments increased 41.8%, from 1.14 ± 0.42 mg/L on day 1 to 1.62 ± 0.48 mg/L on day 10. The reference sediment Fe^{2+} concentrations increased 36.6%, from 4.92 ± 1.44 mg/L on day 1 to 6.72 ± 2.19 mg/L on day 10.

Porewater pH varied more between the hyporheic exposures of the Zn-spiked sediments, compared with the reference sediments ($p < 0.001$; Table 2 and Figure 3C). The pH was on average higher in the Zn-Hyp exposure than in Zn-nonHyp (7.58 ± 0.05 and 7.29 ± 0.04, respectively), whereas Ref-Hyp was more similar to Ref-nonHyp (7.48 ± 0.03 and 7.42 ± 0.03, respectively). The Zn-spiked sediments exhibited greater increase in pH over time, compared with the reference sediments ($p = 0.002$; Table 2). The pH in the Zn-spiked exposures increased from 7.04 ± 0.04 on day 0 to 7.60 ± 0.04 for Zn-nonHyp and to 7.92 ± 0.07 for Zn-Hyp on day 10 (Figure 3C). The reference sediment pH increased less over time, ranging from a pH of 7.31 ± 0.07 on day 0 to 7.67 ± 0.02 in Ref-nonHyp and to 7.78 ± 0.04 Ref-Hyp on day 10. The pH increase over time was likely related to porewater pH equilibration with the surface waters, which had an average pH of 8.12 ± 0.06. The pH in these systems was generally buffered against the release of dissolved metals (Zn^{2+}), because the alkalinity of input water was moderate (~55 mg/L $CaCO_3$).

A significant interaction between hyporheic flow and sediment ($p = 0.002$) is illustrated by the greater difference in porewater Fe between nonhyporheic and hyporheic exposures in the reference sediments (8.29 ± 0.50 mg/L in Ref-nonHyp vs 1.42 ± 0.42 mg/L in Ref-Hyp) compared with the Zn-spiked sediments (1.54 ± 0.14 mg/L in Zn-nonHyp vs 0.32 ± 0.09 mg/L in Zn-Hyp). The effect of the hyporheic treatment was greater in reference than in Zn sediments, likely because porewater Fe was initially higher in the reference (6.04 mg/L ± 0.87 SE) than in the Zn-spiked sediments (1.03 mg/L ± 0.22 SE). Porewater Fe decreased in the hyporheic exposures over time, whereas in the nonhyporheic exposures, porewater Fe increased slightly ($p = 0.003$; Figure 4A). In Ref-Hyp porewater Fe declined by 95.6% (6.09 ± 1.12–0.26 ± 0.11 mg/L) and in Zn-Hyp by 84.3% (1.14 ± 0.38–0.18 ± 0.03 mg/L), whereas in the nonhyporheic exposures, porewater Fe increased over time, by 50.5% in Ref-nonHyp (5.99 ± 1.45–9.02 ± 1.37 mg/L) and by 82.2% in Zn-nonHyp (0.92 ± 0.27–1.68 ± 0.24 mg/L). At the end of the experiment on day 10, porewater Fe was correlated positively with Fe^{2+} ($r = 0.97$, $p < 0.001$) and negatively with dissolved oxygen ($r = –0.52$, $p = 0.008$), indicating decreases in porewater Fe with sediment oxidation.

Porewater Mn concentrations were lower in the hyporheic exposures, relative to the nonhyporheic exposures ($p = 0.024$;

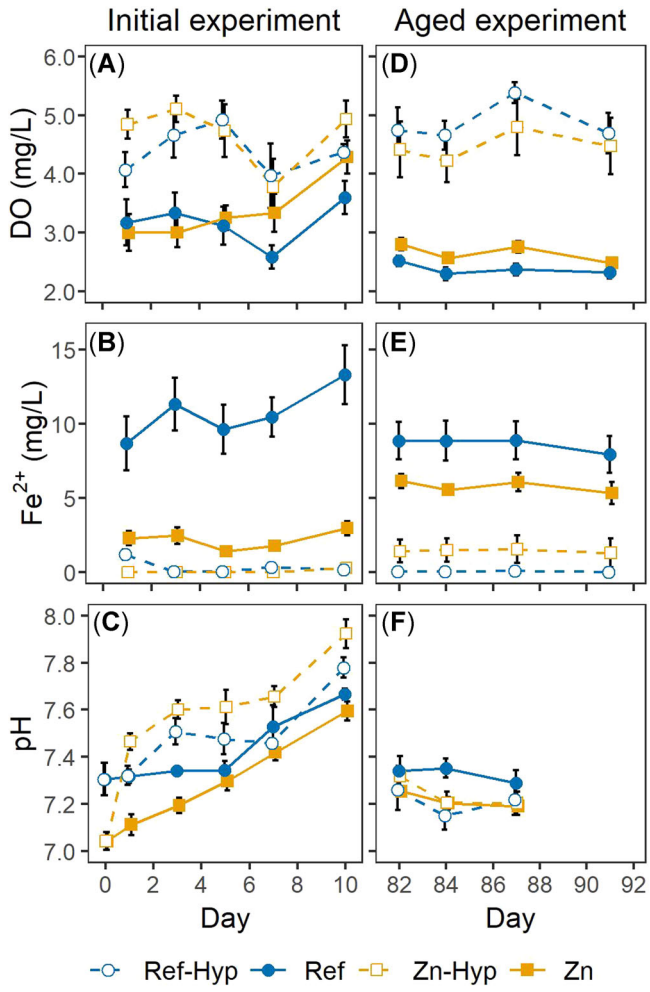

FIGURE 3: Temporal trends in porewater geochemistry during the initial experiment (**A**–**C**) and aged experiment (**D**–**F**). Time is in days on the *x*-axis, and concentrations of porewater chemistry are on the *y*-axis. Graphs include: dissolved oxygen (DO), reduced iron (Fe^{2+}), and pH. Error bars denote ± 1 standard error. A pH meter error on day 9 of the aged experiment prevented pH measurements. Ref-Hyp = reference hyporheic; Ref = reference nonhyporheic; Zn-Hyp = zinc hyporheic; Zn = zinc nonhyporheic.

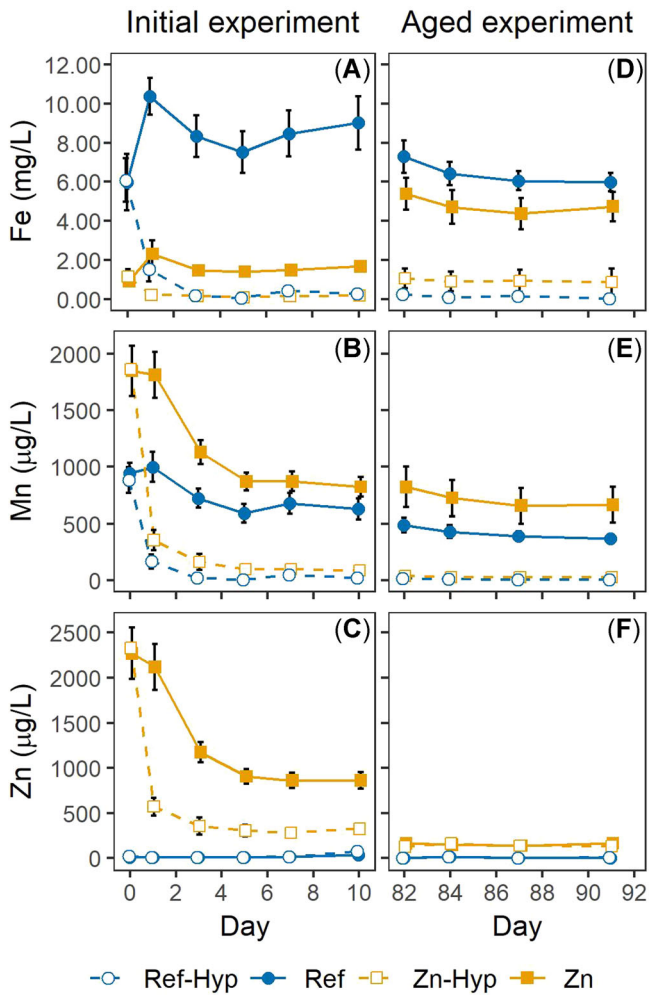

FIGURE 4: Temporal trends in porewater metal chemistry during the initial experiment (**A**–**C**) and the aged experiment (**D**–**F**). Time is in days on the x-axis, and concentrations of porewater metal are on the y-axis. Graphs include: porewater Fe, Mn, and Zn. Error bars denote ± 1 standard error. Ref-Hyp = reference hyporheic; Ref = reference non-hyporheic; Zn-Hyp = zinc hyporheic; Zn = zinc nonhyporheic.

Table 2). Porewater Mn was 74.9% lower in the Ref-Hyp (190.3 ± 56.7 µg/L) than in Ref-nonHyp (759.3 ± 45.2 µg/L), whereas in the Zn-spiked sediments, porewater Mn was 63.1% lower in Zn-Hyp (452.5 ± 120.0 µg/L) than in Zn-nonHyp (1225.9 ± 92.6 µg/L). Hyporheic exposures experienced a greater decline in porewater Mn over time, compared with nonhyporheic exposures ($p = 0.001$; Figure 4B). On day 0 of the experiment, porewater Mn concentrations were their highest, 1855.5 ± 161.4 µg/L in the Zn-spiked sediments and 911.3 ± 70.8 µg/L in the reference sediments. By day 10, the nonhyporheic exposures had experienced moderate declines in porewater Mn, Zn-nonHyp had decreased 55.6% to 823.1 ± 87.2 µg/L, and Ref-nonHyp had declined 31.0% to 629.1 ± 92.3 µg/L. The hyporheic exposures had a greater percentage of decrease, the Zn-Hyp had decreased 95.4% to 84.6 ± 35.8 µg/L, and the Ref-Hyp had decreased 97.7% to 20.7 ± 4.0 µg/L. On day 10, porewater Mn concentrations correlated positively with Fe^{2+} ($r = 0.56$, $p = 0.004$) and negatively with pH ($r = -0.67$, $p < 0.001$).

Porewater Zn was affected by hyporheic exposure, sediment type, and time. There was a larger magnitude of difference in porewater Zn between hyporheic and nonhyporheic exposures in the Zn-spiked sediments, compared with the reference sediments ($p < 0.001$; Table 2 and Figure 4C). Porewater Zn decreased over time in the Zn-spiked exposures only, not in the reference ($p < 0.001$; Figure 4C). Day 0 porewater Zn concentrations averaged 2299.9 ± 228.2 µg/L in the Zn sediments and 12.2 ± 5.1 µg/L in the reference sediments. By day 10, the porewater Zn in the Zn-nonHyp exposure had declined by 62.6% (859.4 ± 91.5 µg/L), and the Zn-Hyp exposure had declined by 85.9% (324.6 ± 54.1 µg/L). Porewater Zn correlated with porewater Mn ($r = 0.56$, $p = 0.005$), and their trends over time were similar (Figure 4A and C).

Total metals were affected by both sediment and hyporheic flows. There was no effect of hyporheic flow on total Fe

($p = 0.406$), but total Fe was higher in the reference sediments (5.28 ± 0.27 g/kg) than in the Zn-spiked sediments (4.21 ± 0.12 g/kg; $p = 0.006$; Table 2). Total Mn was lower in the Zn-spiked sediments than in the reference sediments ($p = 0.013$), and there was no significant hyporheic effect (at $\alpha = 0.05$). Total Zn was lower in the Zn-Hyp exposure (378.7 ± 17.5 mg/kg) compared with the Zn-nonHyp exposure (420.7 ± 11.8 mg/kg; $p = 0.035$), and no differences were observed between the reference exposures. This could be due to a possible loss of total Zn from the system with hyporheic inputs.

Metal-binding ligands were also affected by the hyporheic treatment. Hyporheic exposures had lower AVS than nonhyporheic exposures ($p = 0.027$), but there was no difference in AVS between reference and Zn-spiked sediments ($p = 0.918$). This indicates that regardless of sediment type, AVS was lower in the hyporheic exposures. Despite differences in AVS between the hyporheic treatments, there was no effect of hyporheic treatment on (Zn_{SEM}-AVS)/*f*OC ($p = 0.818$), but the Zn-spiked sediments had higher overall (Zn_{SEM}-AVS)/*f*OC than the reference sediments ($p < 0.001$; Figure 5A).

Amorphous Fe oxide was higher in reference than in Zn-spiked sediments ($p = 0.001$), but there were no differences between hyporheic exposures ($p = 0.399$; Supplemental Data, Table S1). Total oxidized Fe was higher in the nonhyporheic exposure compared with the hyporheic exposure ($p = 0.037$), but was not affected by sediment ($p = 0.253$). Amorphous Mn oxide was unaffected by both treatments, but total and crystalline Mn oxides were both greater in reference sediments than in Zn-spiked sediment ($p = 0.023$ and $p = 0.032$, respectively). The Mn oxides were not affected by hyporheic flow. Zinc bound to amorphous, total, and crystalline Fe/Mn oxides was higher in the Zn-spiked sediments than in the reference sediments ($p < 0.001$, $p < 0.001$, and $p = 0.079$, respectively), and was not affected by hyporheic flow.

The survival of *H. azteca* declined in response to both hyporheic exposure ($p < 0.001$) and Zn-spiked sediment ($p = 0.003$; Figure 6A). The proportion of *H. azteca* survival was highest in the Ref-nonHyp exposures (0.82 ± 0.11) and lowest in the Zn-Hyp exposure (0.00 ± 0.00). In multiple comparison tests, there was no difference in survival between the Ref-Hyp (0.37 ± 0.16) and Zn-nonHyp exposures (0.43 ± 0.11; $p = 0.648$), but both had lower survival than the Ref-nonHyp and higher survival than the Zn-Hyp exposure. The unexpected low survival in the Ref-Hyp exposure, compared with the Ref-nonHyp exposure, was likely due to the visible Fe oxidation on the Ref-Hyp sediments during the 10-d exposure. A thick mat of Fe flocculent developed on the sediment surface in the Ref-Hyp exposure (Supplemental Data, Figure S2). The Fe oxidation did not occur in either of the nonhyporheic exposures or the Zn hyporheic exposure, possibly a product of the sediment spiking procedure and inhibition of Fe-oxidizing microbial communities.

Aged sediment experiment

Porewater redox conditions were more stable over time during the aged sediment experiment. The hyporheic exposures continued to have higher dissolved oxygen than the nonhyporheic exposures, and this relationship was greater for reference than Zn-spiked sediments ($p = 0.003$; Table 3). Dissolved oxygen in Ref-Hyp (4.87 ± 0.15 mg/L) was 105% higher than Ref-nonHyp (2.37 ± 0.05 mg/L), whereas in Zn-spiked sediments, dissolved oxygen in Zn-Hyp (4.47 ± 0.22 mg/L) was only 69% higher than in Zn-nonHyp (2.65 ± 0.05 mg/L; Figure 3D). Dissolved oxygen did not change over time ($p = 0.47$). The Fe^{2+} was also no longer affected by time ($p = 0.14$). The lower Fe^{2+} resulting from hyporheic flows was disproportionately larger in the reference sediments compared with the Zn-spiked

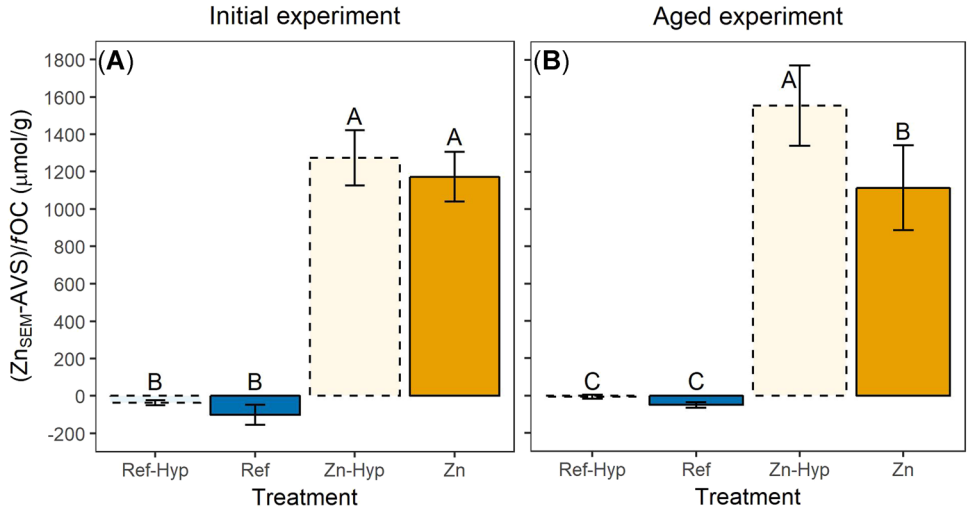

FIGURE 5: Simultaneously extracted metals in excess of acid volatile sulfide normalized for organic carbon (Zn_{SEM}-AVS)/*f*OC (*y*-axis) did not differ between the Zn-nonHyp (labeled Zn) and Zn-Hyp exposures (*x*-axis) on day 10 of the initial experiment (**A**). On day 10 of the aged experiment, the (Zn_{SEM}-AVS)/*f*OC was highest in the Zn-Hyp exposure (**B**). Letters atop error bars denote differences in (Zn_{SEM}-AVS)/*f*OC among exposures within experiments. Ref-Hyp = reference hyporheic; Ref = reference nonhyporheic; Zn-Hyp = Zinc hyporheic; Zn = Zinc nonhyporheic.

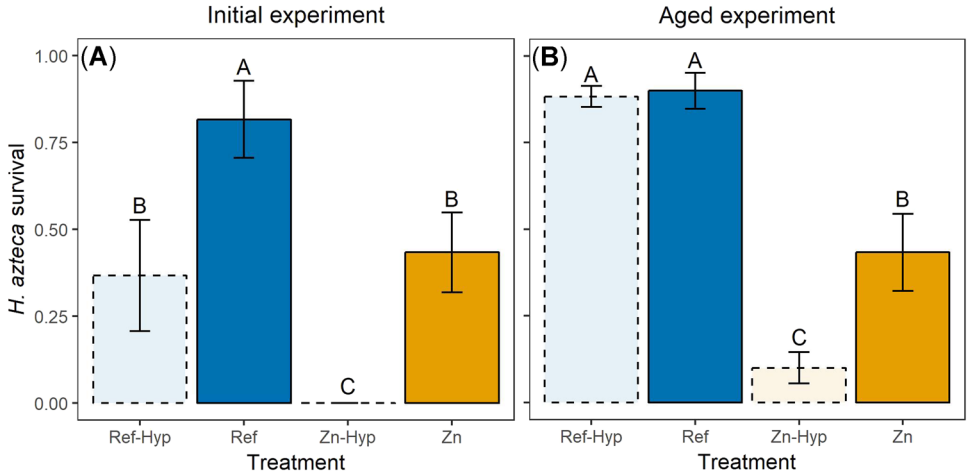

FIGURE 6: *Hyallela azteca* survival (*y*-axis) in the initial (**A**) and aged (**B**) experiments was a function of sediment and hyporheic flow. Letters atop error bars denote differences in survival among exposures within experiments. Ref-Hyp = reference hyporheic; Ref = reference nonhyporheic; Zn-Hyp = Zinc hyporheic; Zn = zinc nonhyporheic.

sediments ($p < 0.001$; Table 3 and Figure 3E). The Ref-Hyp (0.04 ± 0.01 mg/L) was 99.5% lower than the Ref-nonHyp (8.62 ± 0.60 mg/L), whereas the Zn-Hyp (1.43 ± 0.40 mg/L) was 75.2% lower than the Zn-nonHyp (5.78 ± 0.28 mg/L).

Porewater pH returned to the original pH of sediments before the initial experiment, approximately 7.3 (Figure 3F). Porewater pH was relatively higher in the Ref-nonHyp exposure (7.24 ± 0.04) compared with the Ref-Hyp exposure (7.13 ± 0.05), whereas there was little difference in pH between Zn-nonHyp (7.13 ± 0.03) and Zn-Hyp (7.17 ± 0.04) exposures ($p = 0.004$; Table 3). Surface water pH remained high throughout the experiment, at approximately 7.7 to 7.8 in each flume.

The difference between hyporheic exposures on porewater Fe was greater in the reference sediments than in the Zn-spiked sediments ($p < 0.001$; Figure 4D). Porewater Fe was on average 98% lower in Ref-Hyp (0.12 ± 0.03 mg/L) compared with Ref-nonHyp (6.44 ± 0.31 mg/L), whereas in the Zn-spiked sediments, Zn-Hyp (0.94 ± 0.26 mg/L) was 80% lower than Zn-nonHyp (4.80 ± 0.38 mg/L). Porewater Fe also decreased slightly over time across all treatments ($p = 0.034$).

The difference in porewater Mn was relatively higher between the Zn-spiked exposures compared with the reference exposures ($p = 0.001$; Table 3 and Figure 4E). Porewater Mn was 96.0% lower on average in Zn-Hyp (28.5 ± 6.5 µg/L) compared with Zn-nonHyp (717.0 ± 77.5 µg/L), whereas in reference sediments porewater Mn was 80.4% lower in Ref-Hyp (9.2 ± 2.6 µg/L) than in Ref-nonHyp (418.1 ± 25.8 µg/L). Despite the higher Mn concentrations in the nonhyporheic exposures compared with

TABLE 3: Aged experiment linear mixed effects model results for effects of time, hyporheic flow, and Zn-amendment on porewater and sediment chemistry[a]

	Main effects			Interactions		
Endpoints	Time	Hyporheic	Zn	Time × Hyp	Time × Zn	Hyp × Zn
Porewater DO	(–) 0.729	(+) 11.627***	(+) 0.929	1.161	0.017	3.053**
Porewater Fe^{2+}	(–) 1.481	(–) 19.429***	(–) 2.874*	1.187	0.012	8.163***
Porewater pH[b]	(–) 0.767	(–) 2.585*	(–) 1.611	0.139	0.658	2.960**
Porewater Fe	(–) 2.153*	(–) 17.238***	(–) 2.916**	1.297	0.576	5.883***
Porewater Mn[c]	(–) 1.588	(–) 24.869***	(+) 1.110	3.129**	0.755	3.357**
Porewater Zn[c]	(+) 0.864	(+) 0.007	(+) 11.021***	0.027	0.830	0.694
Total Fe	NA	(+) 1.159	(–) 3.545**	NA	NA	0.913
Total Mn	NA	(–) 1.477	(–) 3.382**	NA	NA	0.316
Total Zn	NA	(+) 0.002	(+) 15.424***	NA	NA	0.013
Zn_{SEM}-AVS/*f*OC	NA	(–) 0.751	(+) 8.105***	NA	NA	–4.760**
Zn_{SEM}	NA	(–) 0.077	(+) 10.363***	NA	NA	3.113*
AVS	NA	(–) 2.678	(+) 2.504**	NA	NA	1.952
*f*OC	NA	(+) 1.910	(–) 3.250**	NA	NA	1.831

[a]The *t* value and significance levels are reported, along with a (+) or (–) to indicate directions of main effects (i.e., positive or negative effect of time, hyporheic flow, or Zn-spiked sediment).
[b]Porewater pH was analyzed on days 82, 84, and 87; all other porewater analyses also included measurements on day 91.
[c]Variables were log-transformed due to non-normal distributions.
*$p < 0.05$.
**$p < 0.01$.
***$p < 0.001$.
DO = dissolved oxygen; Zn_{SEM} = zinc fraction of simultaneously extracted metals; AVS = acid volatile sulfides; *f*OC = fraction of organic carbon; NA = not applicable.

the hyporheic exposures, porewater Mn in the hyporheic exposures decreased more over time than the nonhyporheic exposures, relative to starting concentrations in the aged experiment ($p = 0.002$). This relationship was largely driven by the reference sediments; porewater Mn decreased 79.7% in Ref-Hyp compared with 23.7% in Ref-nonHyp, whereas Zn-Hyp decreased 27.0% and Zn-nonHyp declined 19.2% (Figure 4E).

There was no effect of hyporheic flows on porewater Zn in the aged experiment, but the Zn-spiked sediments still maintained higher porewater Zn than the reference sediments ($p < 0.001$; Table 3 and Figure 4F). Porewater Zn concentrations averaged 146.3 ± 10.8 μg/L in the Zn-spiked sediments and were generally at or below detection limits in the reference sediments (< 5.0 μg/L).

Although total metals were unaffected by hyporheic flows (Table 3), redox-sensitive binding ligands were affected by the hyporheic exposure. The interaction between hyporheic flow and sediment type on (Zn_{SEM}-AVS)/*f*OC indicates greater potential Zn bioavailability in the Zn-Hyp exposure compared with the Zn-nonHyp exposure ($p = 0.001$; Table 3). The Zn-Hyp exposure had 39.7% more bioavailable Zn (i.e., (Zn_{SEM}-AVS)/*f*OC) than the Zn-nonHyp exposure (Table 1 and Figure 5B). This relationship is a product of slightly higher Zn_{SEM} and lower *f*OC in the Zn-Hyp exposure, compared with the Zn-nonHyp exposure (Table 3). The Zn_{SEM} was also influenced by an interaction between sediment and hyporheic flows ($p = 0.014$). The AVS was higher in the nonhyporheic sediments than in the hyporheic sediments ($p = 0.028$), driven largely by the lower AVS in Ref-Hyp compared with the other exposures ($p = 0.024$).

Amorphous Fe oxides remained higher in reference than in Zn-spiked sediments ($p < 0.001$), but no effects of treatment were found in total or crystalline Fe oxides (Supplemental Data, Table S1). Amorphous Mn oxides were higher in nonhyporheic exposures, compared with hyporheic ($p = 0.014$), and higher in reference than in Zn-spiked sediments ($p = 0.035$). Multiple comparison tests revealed that this relationship was largely driven by the Zn-Hyp exposure, which had lower amorphous Mn oxide than the Zn-nonHyp ($p < 0.001$), Ref-Hyp ($p = 0.048$), and Ref-nonHyp ($p < 0.001$) exposures. Zinc bound to amorphous, total, and crystalline Fe/Mn oxides was greater in Zn-spiked than in reference sediments for all 3 models ($p < 0.001$, $p < 0.001$, $p = 0.003$, respectively), but was consistently unaffected by hyporheic flow.

Despite no differences in porewater Zn or total Zn in the hyporheic exposures, there was still an effect of hyporheic flows on *H. azteca* survival on day 10. There was a significant interaction between Zn-spiked sediment and hyporheic flows ($p = 0.019$). Although there was no difference in survival between the reference sediments (0.88 ± 0.03 in Ref-nonHyp and 0.90 ± 0.05 in Ref-Hyp), survival in the Zn-Hyp exposure was lower (0.10 ± 0.04) than the in Zn-nonHyp exposure (0.43 ± 0.11; Figure 5B). Throughout the 10-d aged experiment, sediment Zn concentrations (406 ± 19 mg/kg) were lower than the sediment PEC for Zn (459 mg/kg), and porewater Zn concentrations (146 ± 11 μg/L) were just above the PEC for Zn in freshwaters (120 μg/L).

Comparison of initial and aged experiments

Porewater chemistry was more stable during the aged experiment compared with the initial experiment. The pH stabilized to the original pH of the sediments (~7.30), before sediment and hydrologic (surface and hyporheic flow) manipulations, and porewater dissolved oxygen, Fe^{2+}, and pH were constant throughout the 10-d aged experiment. Porewater Zn was also stable over time in the aged experiment, although porewater Fe and Mn still decreased slightly over time. Porewater Zn in the aged experiment was the same for the Zn-Hyp and Zn-nonHyp exposures, indicating that, despite the differences in redox chemistry (Fe^{2+}, pH) and binding capacity (i.e., (Zn_{SEM}-AVS)/*f*OC) there was no longer an effect of hyporheic treatment on porewater Zn.

Survival of *H. azteca* varied between experiments. In the initial experiment, *H. azteca* survival declined in response to hyporheic flow–induced Fe oxidation in the reference sediments, and survival was more negatively correlated with Fe^{2+} ($r = –0.62$, $p = 0.001$), as opposed to other porewater or sediment parameters like (Zn_{SEM}-AVS)/*f*OC ($r = –0.53$, $p = 0.007$), whereas in the aged experiment, there was no visible Fe oxidation in the Ref-Hyp exposure, and survival was high. In the aged experiment, *H. azteca* survival was more correlated with total Zn ($r = –0.86$, $p < 0.001$), (Zn_{SEM}-AVS)/*f*OC ($r = –0.84$, $p < 0.001$), and porewater Zn ($r = –0.59$, $p = 0.003$). Despite similar porewater Zn concentrations in Zn-Hyp and Zn-nonHyp exposures in the aged experiment, there was still decreased survival associated with the Zn-Hyp exposure, relative to Zn-nonHyp exposure. This difference was not related to porewater Zn or total Zn, but may be related to (Zn_{SEM}-AVS)/*f*OC, because it was higher in the Zn-Hyp than in the Zn-nonHyp exposures in the aged experiment (Figure 5B).

DISCUSSION

Hyporheic flow and ecological risk

Our study has established the important role of hyporheic flows on sediment redox chemistry and metal bioavailability. As hypothesized, the Zn-contaminated sediments with hyporheic exposure (Zn-Hyp) were more oxidized than the Zn-contaminated sediments without hyporheic flow (Zn-nonHyp), and they released more Zn from the sediments. This resulted in greater exposure and effects on *H. azteca* in the hyporheic compared with nonhyporheic Zn-contaminated sediments. Although we expected to see *H. azteca* survival increase over time from the initial to the aged experiment, there was little difference in survival between experiments.

These relationships are particularly critical for streams, where downwelling zones in riffles are characterized by oxidized hyporheic sediments (Hendricks and White 1991; Franken et al. 2001), as simulated in our study. Downwelling zones are typically located at the upstream end of riffles in streams and have greater benthic macroinvertebrate community diversity and sensitivity, compared with the downstream ends of riffles (Davy-Bowker et al. 2006), which are characterized by more reduced hyporheic conditions (Boulton 1993). Based on *H. azteca* responses in our study, more sensitive benthic macroinvertebrate

communities residing in downwelling zones could be at higher risk in metal-contaminated streams, compared with benthic communities in upwelling zones, pools, or other stream habitats with limited groundwater–surface water interaction.

The responses of *H. azteca* also showed how metal bioavailability in sediments changes through time in relation to hyporheic flows. Survival in the Zn-spiked treatments of the initial experiment was associated with greater porewater Zn release from Zn-Hyp exposure compared with Zn-nonHyp exposure. Although the initial experiment was not yet in equilibrium (due to changing pH, dissolved oxygen, Fe^{2+}, and dissolved metals over the 10 d), the aged experiment was in equilibrium, because there were few changes in porewater chemistry over the 10-d experiment. Despite the lack of difference in porewater Zn or total Zn concentrations between Zn-Hyp and Zn-nonHyp exposures in the aged experiment, *H. azteca* survival was lower in the Zn-Hyp exposure compared with the Zn-nonHyp exposure. This may be linked to (Zn_{SEM}-AVS)/*f*OC, which was higher in the Zn-Hyp exposure than in the Zn-nonHyp exposure in the aged experiment only, and well above toxic thresholds (~150 µmol/g) for (Zn_{SEM}-AVS)/*f*OC (Burton et al. 2005). The elevated bioavailable Zn likely resulted from the low AVS and *f*OC content in the sediments. In addition, there may have been dietary exposure from the epibenthic feeding. This suggests the potential for long-term effects to biota if SEM is elevated with respect to AVS and organic carbon in downwelling zones.

Although total Fe and Mn were relatively high in these sediments, there were no effects of hyporheic flow on Zn bound to Fe/Mn oxide minerals. In the aged experiment, amorphous Mn oxide was lower in the Zn-Hyp exposure than in the Zn-nonHyp and both reference treatments. This finding suggests a lower capacity in the sediments for Zn to bind to amorphous Mn oxide in the Zn-Hyp exposure, which could potentially contribute to higher *H. azteca* toxicity, although Zn bound to amorphous Fe/Mn oxides was not statistically influenced by hyporheic flow. Formation of Mn oxides in the hyporheic zone is influenced by porewater residence times (Harvey and Fuller 1998), which may have been too short in the present experiment for Mn oxide formation. The effect of hyporheic flow on total oxidized Fe during the initial experiment was likely related to loss of oxidized Fe from the Ref-Hyp exposure during floc formation. In oxidized environments, Fe/Mn oxide minerals are important for metal binding (Danner et al. 2015) and may increase binding within the hyporheic zone specifically (Fuller and Harvey 2000). Future investigations into the role of Fe/Mn oxides as metal-binding ligands in the hyporheic zone are warranted.

Toxicity of the Ref-Hyp exposure during the initial experiment was unexpected, but the significant formation of flocculent mats on the sediment surface suggests that excess Fe oxidation decreased survival. This floc formation was similar to Fe oxidization of groundwater in streams. It is possible that the flocculent caused physical toxicity to *H. azteca* (Vuori 1995). Toxicity could result from excess ingestion as well, because mayflies have been observed physically removing Fe precipitates (Gerhardt 1992). The flocculation effect was also limited to the hyporheic exposure in the reference sediments of the initial experiment, indicating that this was a hyporheic-induced effect. The $ZnCl_2$ spike and subsequent lower pH may have impaired or decreased the Fe-oxidizing microbial communities in Zn-spiked sediments, which was why the Fe flocculent only formed on reference sediments and not on Zn-spiked sediments. In soils, $ZnCl_2$ spiking caused complete inhibition of nitrogen-fixing bacteria at 0.5 mg/L Zn Cl_2 (Cela and Sumner 2002). Porewater Zn concentrations were at 2.0 mg/L at the beginning of our study, suggesting that sediment spiking may be responsible for the lack of Fe oxidation in the Zn-Hyp exposure.

Implications for risk assessment

These findings demonstrate the important role of hyporheic flows on sediment redox chemistry and metal bioavailability. The laboratory experiments provided an assessment of mechanistic effects of Zn-contaminated sediments and oxic hyporheic flows. Whereas other studies have examined the important differences in redox chemistry resulting from hyporheic flows (Hendricks 1993), our study linked hyporheic flow processes with metal fate and biotic effects, which may have important implications for ecological risk assessments in aquatic ecosystems.

Monitoring of hyporheic conditions in metal-contaminated ecosystems is critical to determine whether the hyporheic zone is an important contaminant exposure route, and to understand metal speciation and bioavailability. The USEPA has recommended that these processes be considered in ecological risk assessment and has provided guidance on their incorporation into risk assessment (US Environmental Protection Agency 2008). Hyporheic flow inputs can be measured in the field with the installation of relatively simple equipment. Minipiezometers provide an inexpensive and simple way to measure upwelling and downwelling in shallow sediments via changes in hydraulic head (Winter 1999; Baxter et al. 2003; Rivett et al. 2008). Hyporheic flow direction and magnitude can also be estimated by measuring differences in streambed temperature and depth in the field using a variety of temperature loggers (Hatch et al. 2006; Keery et al. 2007; Gordon et al. 2012). Comparisons of porewater chemistry and contaminant concentrations could then be made among sites with upwelling and downwelling flow and those without hyporheic flow.

As observed in the field study of groundwater–surface water interactions with chlorobenzene toxicity and bioaccumulation (Greenberg et al. 2002), it is important to document hyporheic-related contamination, to link exposures with effects (US Environmental Protection Agency 2008). The present research demonstrates the importance of hyporheic flows on redox-sensitive binding ligands and the subsequent effects on aquatic biological communities. Inclusion of hyporheic flows in ecological risk assessments could more accurately characterize metal exposure pathways to stream aquatic biota.

Supplemental Data—The Supplemental Data are available on the Wiley Online Library at DOI: 10.1002/etc.4554.

Acknowledgment—We thank the following lab staff for their support on this project: S. Nedrich, A. Rentschler, K.

Thiamkeelakul, Y. Li, B. Westmoreland, and T. Hoag. The present study was funded in part by the University of Michigan Graham Sustainability Institute and Rackham Graduate School. The corresponding author is a Postdoctoral Research Fellow in the Institute for Great Lakes Research and Biology Department at Central Michigan University.

Data Availability Statement—Data and associated metadata are available from the corresponding author (harri25a@cmich.edu) or through figshare.com (DOI: 10.6084/m9.figshare.8856260).

REFERENCES

Allen HE, Fu G, Boothman WS, DiToro DM, Mahony JD. 1991. Determination of acid volatile sulfide and selected simultaneously extractable metals in sediment. EPA 821/R-91/100. US Environmental Protection Agency, Washington, DC.

Baker ME, Wiley MJ, Seelbach PW. 2003. GIS-based models of potential groundwater loading in glaciated landscapes: Considerations and development in Lower Michigan. Report 2064. Institute for Fisheries Research, Michigan Department of Natural Resources, Ann Arbor, Michigan, USA.

Bates D, Maechler M, Bolker B, Walker S. 2015. Linear mixed-effects models using. *lme4. J Stat Softw* 67:1–48.

Baxter C, Hauer FR, Woessner WW. 2003. Measuring groundwater–stream water exchange: New techniques for installing minipiezometers and estimating hydraulic conductivity. *Trans Am Fish Soc* 132:493–502.

Boulton AJ. 1993. Stream ecology and surface-hyporheic hydrologic exchange: Implications, techniques and limitations. *Aust J Mar Freshw Res* 44:553–564.

Brunke M, Gonser T. 1997. The ecological significance of exchange processes between rivers and groundwater. *Freshw Biol* 37:1–33.

Burton GA, Nguyen LTH, Janssen C, Baudo R, McWilliam R, Bossuyt B, Beltrami M, Green A. 2005. Field validation of sediment zinc toxicity. *Environ Toxicol Chem* 24:541–553.

Calmano W, Hong J, Forstner U. 1993. Binding and mobilization of heavy metals in contaminated sediments affected by pH and redox potential. *Water Sci Technol Tech* 28:223–235.

Cela S, Sumner ME. 2002. Soil zinc fractions determine inhibition of nitrification. *Water Air Soil Pollut* 141:91–104.

Chapman PM, Wang F, Janssen C, Persoone G, Allen HE. 1998. Ecotoxicology of metals in aquatic sediments: Binding and release, bioavailability, risk assessment, and remediation. *Can J Fish Aquat Sci* 55:2221–2243.

Cooper MJ, Rediske RR, Uzarski DG, Burton TM. 2001. Sediment contamination and faunal communities in two subwatersheds of Mona Lake, Michigan. *J Environ Qual* 38:1255–1265.

Costello DM, Hammerschmidt CR, Burton GA. 2015. Copper sediment toxicity and partitioning during oxidation in a flow-through flume. *Environ Sci Technol* 49:6926–6933.

Danner KM, Hammerschmidt CR, Costello DM, Burton GA. 2015. Copper and nickel partitioning with nanoscale goethite under variable aquatic conditions. *Environ Toxicol Chem* 34:1705–1710.

Davy-Bowker J, Sweeting W, Wright N, Clarke RT, Arnott S. 2006. The distribution of benthic and hyporheic macroinvertebrates from the heads and tails of riffles. *Hydrobiologia* 563:109–123.

Feris K, Ramsey P, Frazar C, Moore JN, Gannon JE, Holben WE. 2003. Differences in hyporheic-zone microbial community structure along a heavy-metal contamination gradient. *Appl Environ Microbiol* 69:5563–5573.

Feris KP, Ramsey PW, Gibbons SM, Frazar C, Rillig MC, Moore JN, Gannon JE, Holben WE. 2009. Hyporheic microbial community development is a sensitive indicator of metal contamination. *Environ Sci Technol* 43:6158–6163.

Franken RJM, Storey RG, Williams DD. 2001. Biological, chemical and physiucal characteristics of downwelling and upwelling zones in the hyporheic zone of a north-temperature stream. *Hydrobiologia* 444:183–195.

Fuller CC, Harvey JW. 2000. Reactive uptake of trace metals in the hyporheic zone of a mining-contaminated stream, Pinal Creek, Arizona. *Environ Sci Technol* 34:1150–1155.

Gerhardt A. 1992. Effects of subacute doses of iron (Fe) on *Leptophlebia marginata* (Insecta: Ephemeroptera). *Freshw Biol* 27:79–84.

Gibert J, Plénet S, Marmonier P, Vanek V. 1995. Hydrological exchange and sediment characteristics in a riverbank: Relationship between heavy metals and invertebrate community structure. *Can J Fish Aquat Sci* 52:2084–2097.

Gordon RP, Lautz LK, Briggs MA, McKenzie JM. 2012. Automated calculation of vertical pore-water flux from field temperature time series using the VFLUX method and computer program. *J Hydrol* 420–421:142–158.

Greenberg MS, Burton GA, Rowland CD. 2002. Optimizing interpretation of in situ effects of riverine pollutants: Impact of upwelling and downwelling. *Environ Toxicol Chem* 21:289–297.

Harvey JW, Fuller CC. 1998. Effect of enhanced manganese oxidation in the hyporheic zone on basin-scale geochemical mass balance. *Water Resour Res* 34:623.

Hatch CE, Fisher AT, Revenaugh JS, Constantz J, Ruehl C. 2006. Quantifying surface water-groundwater interactions using time series analysis of streambed thermal records: Method development. *Water Resour Res* 42. DOI:10.1029/2005WR004787

Hendricks SP. 1993. Microbial ecology of the hyporheic zone: A perspective integrating hydrology and biology. *J North Am Benthol Soc* 12:70–78.

Hendricks SP, White DS. 1991. Physicochemical patterns within a hyporheic zone of a Northern Michigan river, with comments on surface water patterns. *Can J Fish Aquat Sci* 48:1645–1654.

Hendricks SP, White DS. 2000. Stream and groundwater influences on phosphorous biogeochemistry. In Jones JB, Mulholland PJ, eds, *Streams and Groundwaters*. Academic, San Diego, CA, USA, pp 221–235.

Hothorn T, Bretz F, Westfall P. 2008. Simultaneous inference in general parametric models. *Biometrical J* 50:346–363.

Hutchins CM, Teasdale PR, Lee SY, Simpson SL. 2009. The effect of sediment type and pH-adjustment on the porewater chemistry of copper- and zinc-spiked sediments. *Soil Sediment Contam* 18:55–73.

Keery J, Binley A, Crook N, Smith JWN. 2007. Temporal and spatial variability of groundwater-surface water fluxes: Development and application of an analytical method using temperature time series. *J Hydrol* 336:1–16.

Kostka JE, Luther GW. 1994. Partitioning and speciation of solid phase iron in saltmarsh sediments. *Geochim Cosmochim Acta* 58:1701–1710.

Kuznetsova A, Brockhoff PB, Christensen RHB. 2017. Package: Tests in linear mixed effects models. *J Stat Softw* 82:1–26.

MacDonald DD, Ingersoll CG, Berger TA. 2000. Development and evaluation of consensus-based sediment quality guidelines for freshwater ecosystems. *Arch Environ Contam Toxicol* 39:20–31.

Mathers KL, Millett J, Robertson AL, Stubbington R, Wood PJ. 2014. Faunal response to benthic and hyporheic sedimentation varies with direction of vertical hydrological exchange. *Freshw Biol* 59:2278–2289.

Mendonca RM, Daley JM, Hudson ML, Schlekat C, Burton GA, Costello D. 2017. Metal oxides in surface sediment control nickel bioavailability to benthic macroinvertebrates. *Environ Sci Technol* 51:13407–13416.

Moldovan OT, Levei E, Marin C, Banciu M, Banciu HL, Pavelescu C, Brad T, Cîmpean M, Meleg I, Iepure S, Povara I. 2011. Spatial distribution patterns of the hyporheic invertebrate communities in a polluted river in Romania. *Hydrobiologia* 669:63–82.

Morrice JA, Valett HM, Dahm CN, Campana ME. 1997. Alluvial characteristics, groundwater-surface water exchange and hydrological retention in headwater streams. *Hydrol Process* 11:253–267.

Munn NL, Meyer JL. 1988. Rapid flow through the sediments of a headwater stream in the southern Appalachians. *Freshw Biol* 20:235–240.

Nelson SM, Roline RA. 1999. Relationships between metals and hyporheic invertebrate community structure in a river recovering from metals contamination. *Hydrobiologia* 397:211–226.

Olsen DA, Townsend CR. 2003. Hyporheic community composition in a gravel-bedstream: Influence of vertical hydrological exchange, sediment structure and physicochemistry. *Freshw Biol* 48:1363–1378.

Rehg KJ, Packman AI, Ren J. 2005. Effects of suspended sediment characteristics and bed sediment transport on streambed clogging. *Hydrol Process* 19:413–427.

Rivett MO, Ellis PA, Greswell RB, Ward RS, Roche RS, Cleverly MG, Walker C, Conran D, Fitzgerald PJ, Willcox T, Dowle J. 2008. Cost-effective mini drive-point piezometers and multilevel samplers for monitoring the hyporheic zone. *Q J Eng Geol Hydrogeol* 41:49–60.

RStudio Team. 2018. *RStudio: Integrated Development for R*. RStudio, Boston, MA, USA. [cited 2018 September 12]. Available from: http://www.rstudio.com/

Simpson SL, Angel BM, Jolley DF. 2004. Metal equilibration in laboratory-contaminated (spiked) sediments used for the development of whole-sediment toxicity tests. *Chemosphere* 54:597–609.

Steinman A, Rediske R, Denning R, Nemeth L, Uzarski D, Biddanda B, Luttenton M. 2003. Preliminary watershed assessment: Mona Lake Watershed. Scientific Technical Report 9. Community Foundation for Muskegon County, Muskegon, Michigan, USA.

Stookey LL. 1970. Ferrozine—A new spectrophotometric reagent for iron. *Anal Chem* 42:779–781.

US Environmental Protection Agency. 2008. Evaluating ground-water/surface-water transition zones in ecological risk assessment. EPA-540-R06-072. Washington, DC.

US Environmental Protection Agency. 1996. Method 3050B: Acid digestion of sediments, sludges, and soils. Revision 2. Washington, DC.

Vuori K-M. 1995. Direct and indirect effects of iron on river ecosystems. *Ann Zool Fennici* 32:317–329.

Winter TC. 1999. Relation of streams, lakes, and wetlands to groundwater flow systems. *Hydrogeol J* 7:28–45.

Zaramella M, Marion A, Packman AI. 2006. Applicability of the transient storage model to the hyporheic exchange of metals. *J Contam Hydrol* 84:21–35.

